

Tensile fracture behavior of continuous SiC fiber-reinforced SiC matrix composites at elevated temperatures and correlation to in situ constituent properties

Shuqi Guo^{*,1}, Yutaka Kagawa

Institute of Industrial Science, The University of Tokyo, 7-22-1, Roppongi, Minato-ku, Tokyo 106-8558, Japan

Received 21 March 2001; received in revised form 20 December 2001; accepted 6 January 2002

Abstract

The tensile fracture behavior and tensile mechanical properties of polymer infiltration pyrolysis (PIP)-processed two-dimensional plain-woven fabric carbon-coated NicalonTM SiC fiber and BN-coated Hi-NicalonTM SiC fiber-reinforced SiC matrix composites have been investigated. Tensile testing of the composites was carried out in air between 298 and 1400 K. In situ fiber strength and interface shear stress were determined by fracture mirror size and pulled-out fiber length measurements. For the Nicalon/C/SiC, tensile strength remained nearly constant up to 800 K, and while the strength dropped from 140 MPa at 800 K to 41 MPa at 1200 K, with weakest link failure mode. For the Hi-Nicalon/BN/SiC, the tensile strength increased slightly with increase in test temperature up to 1200 K; however, a large decrease in the strength was observed at 1400 K. In the case of the Hi-Nicalon/BN/SiC, the fracture was governed by fiber bundle strength. The temperature dependence of tensile strength and fracture behavior of both composites was attributed to change of the in situ constituent properties with temperature. © 2002 Elsevier Science Ltd. All rights reserved.

Keywords: Composites; Fiber strength; Interface shear stress; Mechanical properties; Polymer infiltration pyrolysis; SiC/SiC

1. Introduction

Continuous fiber-reinforced ceramic matrix composites (CFCCs) have become an important class of materials for structural applications at elevated temperatures because of their improved flaw tolerance, large fracture resistance, and noncatastrophic mode of failure comparing with monolithic ceramic materials. Among CFCCs, SiC fiber-reinforced SiC matrix composites have been studied extensively in recent years because the SiC fiber shows a potential for applications at elevated temperatures. These studies demonstrated that the tensile mechanical behavior and properties of the composites strongly depend on the in situ fiber strength characteristics, interface properties and matrix cracking stress, as well as the fabrication processes.^{1–5}

The damage evolution of the composites usually includes two fundamental regimes: (i) at lower stresses, matrix cracking originating from defects in the matrix and followed by interface debonding between the fiber and matrix, and (ii) at higher stresses, occurrence of fiber damage and ultimate failure.^{6,7} If matrix cracking can reach the fully-saturated state prior to composite failure, the subsequent deformation and failure are dominated entirely by the fiber flaw population, showing a noncatastrophic failure.^{6,7} However, if the fibers are sufficiently weak and interface bonding comparatively strong due to interface reaction in an oxidizing environment at high temperatures, composite failure is also possible in the regime of matrix cracking, showing a catastrophic fracture similar to the fracture of a monolithic ceramic.^{8,9} The transition from noncatastrophic to catastrophic fracture depends on in situ constituent properties. Thus, it is important to understand this transition to clarify tensile fracture behavior of the composites and to allow correlation with the in situ constituent properties. In situ constituent properties of the composites such as fiber strength, interface shear

* Corresponding author. Fax: +81-0298-51-3613.

E-mail address: guo.shuqi@nims.go.jp (S. Guo).

¹ National Institute for Materials Science, 1-1 Namiki, Tsukuba, Ibaraki 305-0044, Japan.

stress and matrix cracking stress, can be determined by a tensile test and fractographic analysis and measurements.^{10,11} Thus, it is possible to evaluate correlation of the mechanical behavior to in situ constituent properties. Although the correlation of tensile fracture behavior to in situ constituent properties has been reported in CVI-processed composites,^{3,12} this correlation for PIP-processed composites is not well known. In the present study, tensile testing of the two PIP-processed SiC fiber-reinforced SiC matrix composites was carried out at room and elevated temperatures. The matrix cracking stress, in situ fiber strength and interface shear stress were obtained. The correlation of the tensile fracture behavior of the composites to in situ constituent properties was discussed.

2. Experimental procedure

2.1. Composite materials

The composite materials used in the present study were 2D plain-woven fabric SiC fiber–SiC matrix composites fabricated by the PIP process. To compare the effect of fiber strength and interface properties on the tensile fracture behavior of the composites, NicalonTM and Hi-NicalonTM SiC fibers (Nippon Carbon Co. Ltd., Tokyo, Japan) in which the surfaces were respectively coated with $\approx 0.04 \mu\text{m}$ amorphous carbon and $\approx 0.4 \mu\text{m}$ BN by chemical vapor deposition (CVD) were used as reinforcements. The typical properties and chemical composition of the two fibers are listed in Table 1.¹³ The coated SiC fibers were formed a plain-woven fabric sheet, with 16×16 numbers of fiber per inch. The fabric sheets averaging $150 \times 150 \text{ mm}$ in size were cut from the formed plane-woven sheet. The cut fabric sheets were infiltrated with a polycarbosilane solution containing a fine β -SiC powder. The fine β -SiC powder had an average diameter of $\approx 4 \mu\text{m}$ and its addition effectively reduced pore content in the SiC matrix after pyrolysis.^{4,5}

Table 1
Typical properties and chemical composition of the two fibers

Fibres		Nicalon TM SiC	Hi-Nicalon TM SiC
Fibre properties			
Tensile strength	(GPa)	3.0	2.8
Young's modulus	(GPa)	220	270
Elongation	(%)	1.4	1.0
Average fibre radius	(μm)	7	7
Number of fibres per bundles		500	500
Chemical compositions			
Si	(wt.%)	56.6	62.4
C	(wt.%)	31.7	37.1
O	(wt%)	11.7	0.5

The polycarbosilane had a melting point of 514 K, an average molecular weight of ≈ 2410 , and its chemical composition was: 60 mass% Si, 40 mass% C, <1 mass% O. The five infiltrated pre-preg sheets were stacked and pressed, and the stacked sheets were then cured at 523 K in ambient air to obtain the composite precursor. The composite precursor was pyrolyzed at 1273 K in a high purity N_2 atmosphere. Approximately 40 vol.% of pores existed in the pyrolyzed composite due to the low yield weight of the polycarbosilane. To further reduce the porosity of the composite, a multiple PIP process was applied. After 10 PIP cycles, the total fiber volume fraction, f , and the total porosity of the composite were ≈ 0.28 and ≈ 0.09 , respectively. Hereafter, the NicalonTM SiC fiber and Hi-NicalonTM SiC fiber-reinforced SiC matrix composites fabricated are denoted as Nicalon/C/SiC and Hi-Nicalon/BN/SiC, respectively.

2.2. Tensile test

The composite panels were cut into a dog-bone type tensile test specimen with the long axis parallel to one of the fiber axis directions. The shape and dimensions of the specimen for monotonic tension testing are shown in Fig. 1. Quasi-static monotonic tensile testing was carried out using a servo-hydraulic MTS 808 testing system (MTS System Co., MI, USA) with a constant crosshead displacement rate of 0.5 mm/min in ambient air at room temperature (298 K), 800, 1200 and 1400 K. Three composite specimens were used for each measurement. An electric furnace attached to the MTS testing system provided the heating. Axial strain was measured directly from the gauge length of the specimen by using a contact extensometer (MTS Model 632.59, MTS System Co., MI). Before the loading, the specimen was heated

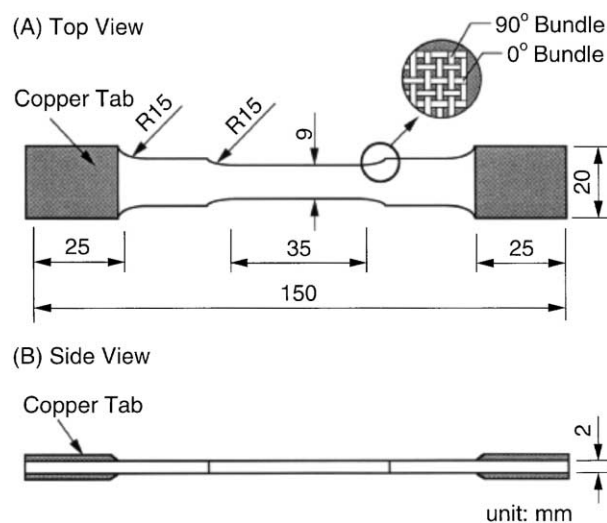


Fig. 1. Shape and dimensions of the specimen for monotonic tension testing.

to the test temperature at a rate of 50 °C/min and then held for ≈ 10 min to give a uniform temperature distribution in the specimen. After the tension testing, the fracture surfaces of the specimens were characterized using an optical microscope and scanning electron microscope (SEM).

2.3. In situ fiber strength and effective interface shear stress

(i) *In situ fiber strength*: in situ fiber strength in the composite, σ_{fu} , was estimated from the fracture mirror radius, r_m , of a pulled-out fiber.¹⁰ The tensile strength, σ_{fu} , of the fiber is given by:¹⁰

$$\sigma_{fu} = \frac{3.5K_f}{\sqrt{r_m}} \quad (1)$$

where K_f is the (mode I) fracture toughness of the fiber. The fracture toughness of the SiC fiber is reported to be $\approx 1.0 \text{ MPa m}^{1/2}$.¹⁴ This value is assumed to be independent of the test temperature because only a slight dependence up to 1100 K has been observed for Nicalon™ SiC fiber.¹⁴ Assuming that the fiber failure follows the weakest-link principle, the statistical distribution of fiber strength is described according to Weibull's two-parameter statistical distribution theory.¹⁵ Failure probability of the fiber, which is associated with fiber strength, is obtained using the mean rank method.

(ii) *Interface shear stress*: interface shear stress, τ_i , of SiC fiber-reinforced ceramic matrix composites is expressed using an average fiber pullout length, L , as^{14,16}

$$\tau_i = \frac{\lambda(m)R_f\sigma_{fu}}{4L} \quad (2)$$

where the R_f is the radius of fiber ($\sim 7 \mu\text{m}$), $\lambda(m)$ is a nondimensional function determined from the statistics of fiber failure properties and takes a value close to unity for $m > 3$.¹⁷ The interface shear stress determined represents the load transverse capacity from the fiber to the matrix, reflecting the interface sliding resistance in the debonding interface.

3. Results

3.1. Tensile mechanical behavior

(i) *Tensile stress–strain curves*: Fig. 2 shows the typical tensile stress–strain curves of the Nicalon/C/SiC at room and elevated temperatures. All the curves exhibit a linear response near the origin and a following gradual decrease of the slope up to fracture, i.e. nonlinear

response. The large nonlinear regime is observed and remains nearly constant up to 800 K; however, this regime is sharply reduced at 1200 K and nearly disappears, showing a brittle fracture similar to that of monolithic ceramics. Fig. 3 shows the typical tensile stress–strain curves of the Hi-Nicalon/BN/SiC at room and elevated temperatures. The curves show a tensile stress–strain behavior similar to that of the Nicalon/C/SiC; the linear deformation regime and nonlinear deformation regime are present, but the nonlinear regime is larger for all the test temperatures compared to the Nicalon/C/SiC, showing a larger fracture resistance, especially at and above 1200 K.

The Young's modulus of the composite, E_c , was obtained from the initial slope of these curves. The apparent matrix cracking stress, σ_{mc} , was determined at the transition point from a linear response to a nonlinear response, because the deviation from linear behavior is often attributed to initiation of the matrix cracking.^{18,19} However, studies have shown that matrix

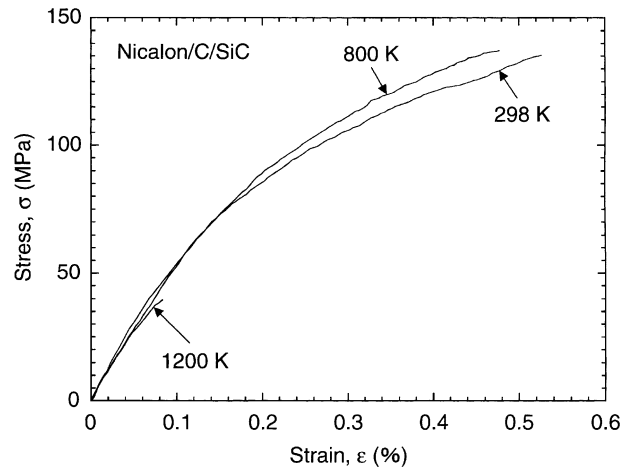


Fig. 2. Typical monotonic tensile stress–strain curves of the Nicalon/C/SiC at room and elevated temperatures.

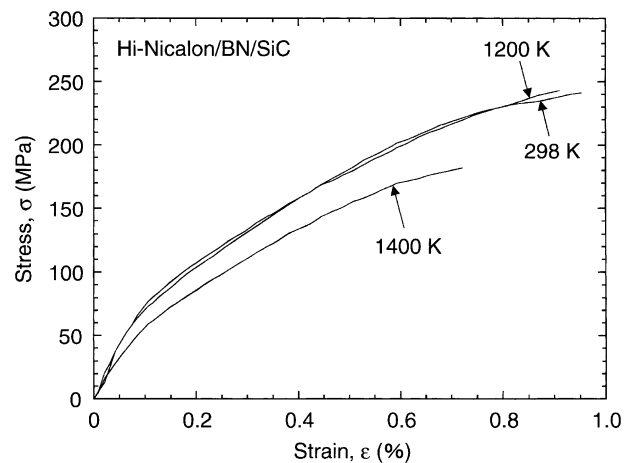


Fig. 3. Typical monotonic tensile stress–strain curves of the Hi-Nicalon/BN/SiC at room and elevated temperatures.

cracking usually initiates well below this stress.^{20,21} Thus, in the present study, the apparent matrix cracking stress obtained should be higher than the true matrix cracking stress. The matrix cracking behavior clearly was observed in the polished longitudinal cross-section of the composite specimens tested at room and elevated temperatures (Fig. 4). The transverse matrix cracks are formed through the transverse fiber bundle, and some of them are arrested at the interface between the longitudinal and transverse fiber bundles.

The average values of E_c and σ_{mc} that were calculated from the duplicate tests at each temperature are shown in Table 2, together with the tensile strength, σ_{TS} , and the strain to failure, ϵ_c . For the Nicalon/C/SiC, the tensile mechanical properties remain nearly constant from 298 to 800 K and that they degrade sharply by 1200 K, in particular, the tensile strength and strain to failure dropped from 140 MPa and 0.38% at 800 K to 41 MPa and 0.075% at 1200 K. For the Hi-Nicalon/BN/SiC, on the other hand, the mechanical properties such as E_c , σ_{mc} , ϵ_c and σ_{TS} remain nearly constant up to 1200 K and begin to degrade at 1400 K; they are much higher than those of the Nicalon/C/SiC at all test temperatures.

(ii) *Fracture surface observations:* Fig. 5 shows the macroscopic fracture appearance of the Nicalon/C/SiC

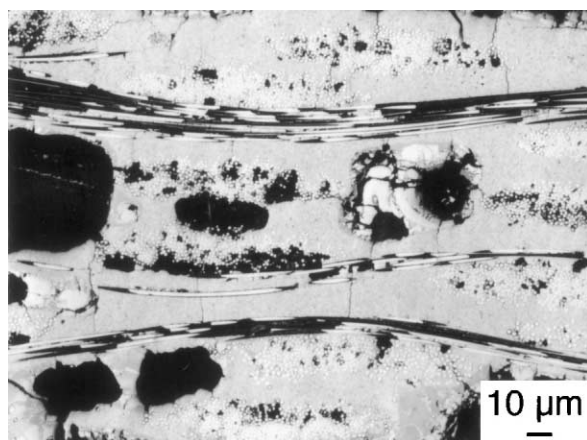


Fig. 4. An example of optical photographs of polished longitudinal cross-section of the two composites after monotonic tension testing, showing matrix cracking ($T = 298$ K, Hi-Nicalon/BN/SiC).

tested at room and elevated temperatures. The pulled-out fibers are observed in the composite specimens fractured at and below 800 K, however, this fiber pull-out behavior is not seen in the composite tested at 1200 K, showing a brittle fracture fashion. Fig. 6 shows the macroscopic fracture appearances of the Hi-Nicalon/BN/SiC tested at room and elevated temperatures. Differing from the Nicalon/C/SiC, the room temperature fracture behavior of the Hi-Nicalon/BN/SiC shows a fracture path which is jagged and stepped across the thickness, and there is extensive fiber and fiber tow pull-out. Although the fracture surface became smoother with increasing test temperature, the pulled-out fibers are observed over all test temperatures.

Fig. 7 shows SEM micrographs of the fracture surfaces of both the composites. Although all fracture surfaces of the composites tested at room and high temperatures showed a fibrous fracture surface, only few and short pulled-out fibers are observed in the fracture surface of the Nicalon/C/SiC tested at 1200 K. This is probably attributed to the silica (SiO_2) formation at the interface by oxidation of both the matrix and fiber, because of air penetration into the gaps at the interface resulting from the elimination of the C-coating layer by oxidation above 700 K.^{22,23} The pulled-out length of fiber was measured using the method reported elsewhere.³ For the Nicalon/C/SiC, the average pulled-out fiber length is ≈ 50 μm at 298 K, ≈ 70 μm at 800 K and ≈ 20 μm at 1200 K. For the Hi-Nicalon/BN/SiC, the pulled-out fiber length is ≈ 300 μm at 298 K, ≈ 250 μm at 1200 K and ≈ 190 μm at 1400 K. It is clear that the pulled-out fiber length of the Hi-Nicalon/BN/SiC is much larger than that of the Nicalon/C/SiC at room and elevated temperatures. Moreover, for the Nicalon/C/SiC tested at and below 800 K there are regions in all the bundles in which the fiber-fracture locations are essentially coplanar with one another compared to the Hi-Nicalon/BN/SiC.

3.2. In situ fiber strength

The in situ fiber strength characteristics of the NicalonTM SiC fiber and the Hi-NicalonTM SiC fiber were obtained using Eq. (1) and the results are summarized in

Table 2
Tensile experimental results of both the Nicalon/C/SiC and Hi-Nicalon/BN/SiC

Composite materials	Test temperature T (K)	Young's modulus E_c (GPa)	Apparent matrix cracking stress σ_{mc} (MPa)	Measured tensile strength σ_{TS} (MPa)	Strain to failure ϵ_c (%)	Predicted tensile strength σ_{TS}
Nicalon/C/SiC	298	58 ± 5	65 ± 8	136 ± 19	0.42 ± 0.1	177
	800	55 ± 4	55 ± 5	140 ± 12	0.38 ± 0.08	175
	1200	49 ± 4	33 ± 3	41 ± 5	0.075 ± 0.015	127
Hi-Nicalon/BN/SiC	298	80 ± 5	75 ± 9	226 ± 11	0.84 ± 0.12	223
	1200	76 ± 4	70 ± 7	237 ± 6	0.9 ± 0.06	228
	1400	60 ± 3	50 ± 5	197 ± 15	0.68 ± 0.09	209

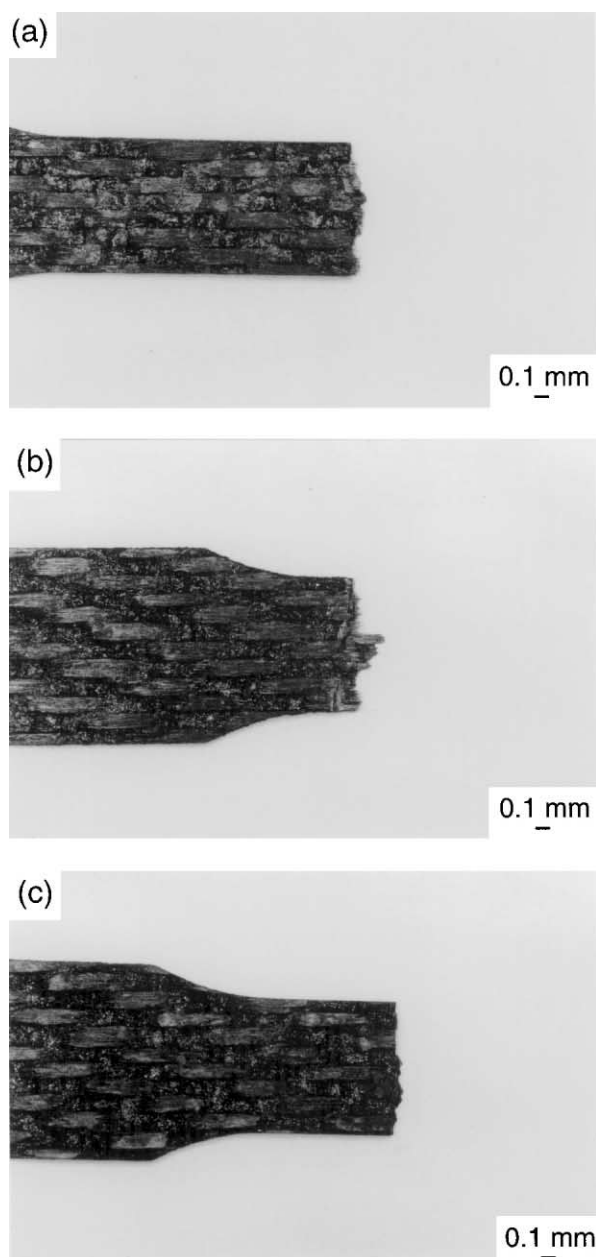


Fig. 5. Macroscopic fracture appearance of the Nicalon/C/SiC tested at (a) 298 K, (b) 800 K and (c) 1200 K.

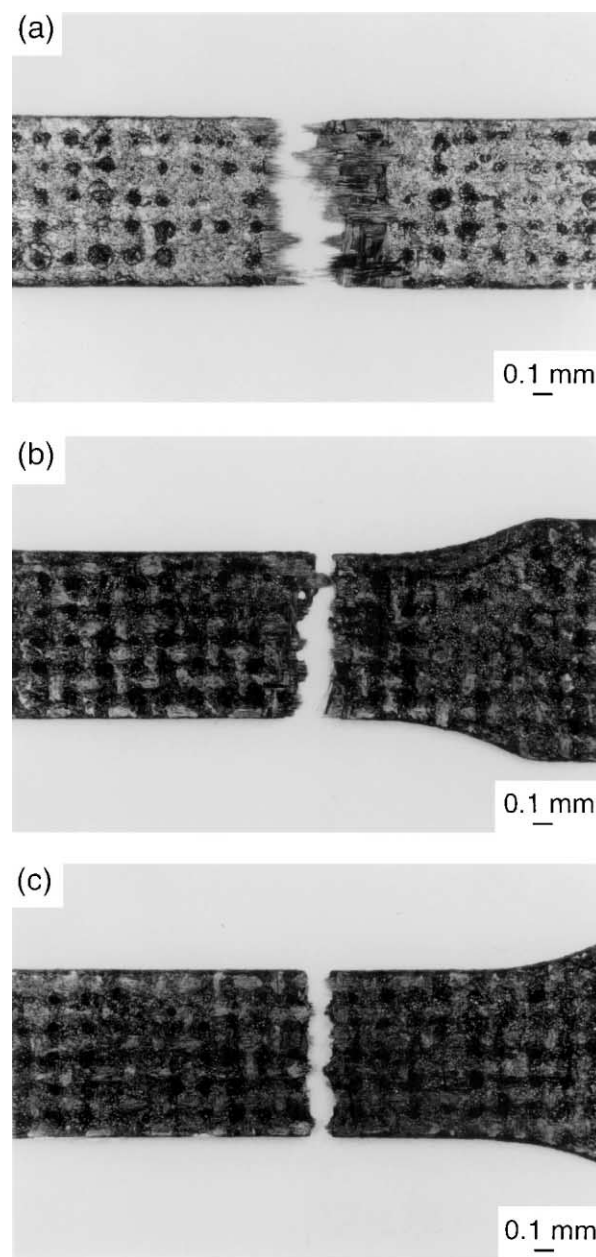


Fig. 6. Macroscopic fracture appearance of the Hi-Nicalon/BN/SiC tested at (a) 298 K, (b) 1200 K and (c) 1400 K.

Table 3. The in situ strength of NicalonTM SiC fiber is 1765 MPa at 298 K and 1705 MPa at 800 K; however, it decreases to 1235 MPa at 1200 K. The degradation of fiber strength due to exposure to high temperatures is already documented in the literature.^{24,25} The fiber strength decreased ~ 30 and $\sim 70\%$, respectively, after exposure at 1273 and 1573 K for 12 h in wet-air atmosphere,²⁴ and the tensile strength drops from 2000 MPa at room temperature to 1000 MPa at 1573 K in air.²⁵ This reduction is explained by the microstructural and stoichiometric changes and void formation in the fiber at higher temperatures. Similar changes, although not as severe because of a short-term heat exposure at

elevated temperature, are expected for the carbon-coated NicalonTM fibers investigated in the present study, especially microstructural and stoichiometric changes of the fiber. On the other hand, the in situ strength of Hi-NicalonTM SiC fiber remains nearly the same value at the temperatures of 298 and 1200 K, and it begins to decrease above 1200 K. The fiber strength at 1400 K is lower by $\approx 11\%$, compared to that at room temperature. Strength decrease of the Hi-NicalonTM SiC fiber at high temperature has been documented in the literature.²⁶ Degradation in the strength of the fiber above the temperature of 1573 K in ambient air was observed and the major reason given for this was grain

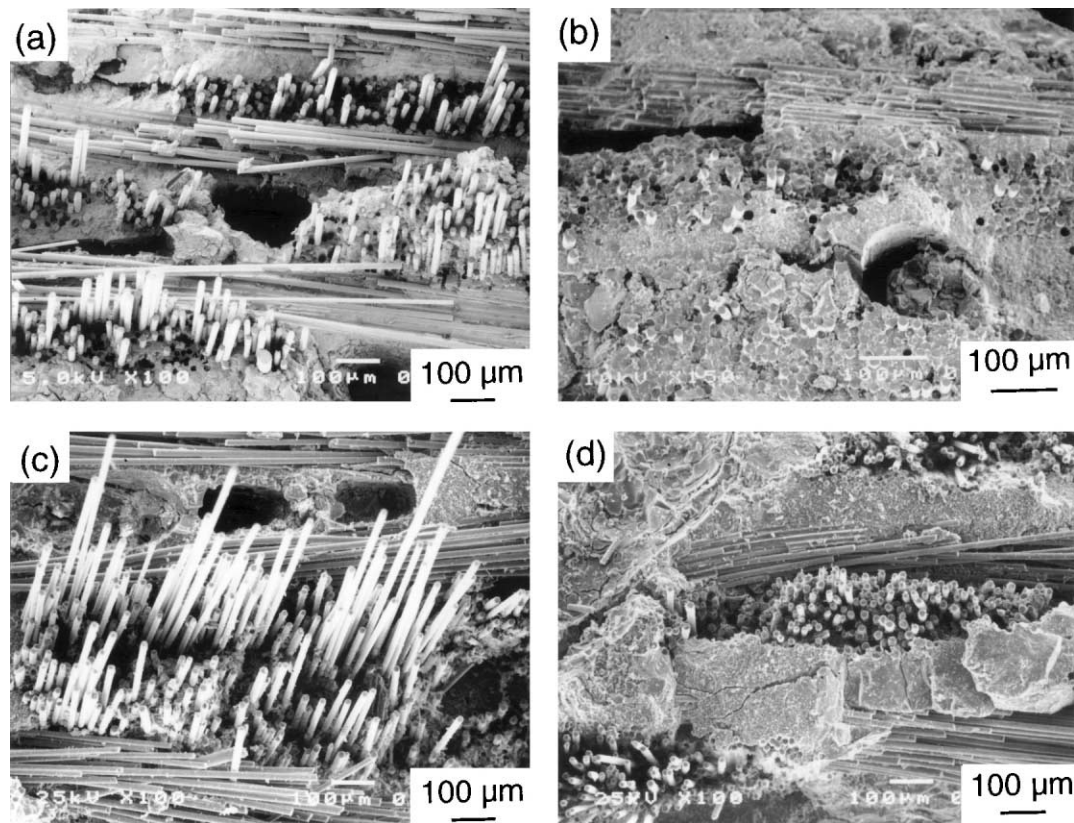


Fig. 7. Scanning electron micrographs of fracture surfaces of the Nicalon™ SiC/C/SiC tested at (a) 298 K, and (b) 1200 K and the Hi-Nicalon/BN/SiC tested at (c) 298 K, and (d) 1400 K.

Table 3

In situ fiber tensile strength characteristics and interface shear stress of both the Nicalon/C/SiC and Hi-Nicalon/BN/SiC at room and elevated temperatures

Composite materials	Test temperature T (K)	In situ fibre strength σ_{fu} (MPa)	Weibull modulus m	Fibre pullout length L (μm)	Interfacial shear stress τ_i (MPa)	Number of measurements
Nicalon/C/SiC	298	1765	6.2	50 ± 35	59 ± 7	70
	800	1705	6.7	70 ± 40	44 ± 10	70
	1200	1235	6.9	20 ± 10	126 ± 15	70
Hi-Nicalon/BN/SiC	298	2199	8.7	300 ± 140	13 ± 5	70
	1200	2187	9.1	250 ± 110	15 ± 5	70
	1400	1961	9.6	190 ± 90	17 ± 7	70

growth.²⁶ Nearly the same temperature dependence was observed as in the present study.

3.3. Interface shear stress

The Interface shear stresses of the Nicalon/C/SiC and the Hi-Nicalon/BN/SiC composites are obtained using Eq. (2), and the results are also summarized in Table 3. For the Nicalon/C/SiC, the interfacial shear stress is 59 MPa at 298 K, 44 MPa at 800 K and 126 MPa at 1200 K. The interfacial shear stress decreases at 800 K from that of 298 K and then increases again at 1200 K. For the Hi-Nicalon/BN/SiC, the interface shear stress tends to increase with increasing test temperature, and the

values at room and elevated temperatures are much lower than those of the Nicalon/C/SiC. This should be attributed to a better oxidation resistance of BN-coating on the Hi-Nicalon™ fiber surface than C-coating on Nicalon™ fiber surface.^{22,23}

4. Discussion

The experimental results indicated that the tensile fracture behavior and properties of both the Nicalon/C/SiC and the Hi-Nicalon/BN/SiC depended on test temperature. The temperature dependence essentially originates from the change of in situ constituent properties

with test temperature. Assuming that the fiber stress is uniform and the fiber failure is non-interactive, the tensile strength of the composites, σ_{TS} , is approximately given by²⁷

$$\sigma_{TS} = f_L \sigma_{bu} \quad (3a)$$

$$\sigma_{bu} = \left(\frac{1}{me} \right)^{1/m} \frac{\sigma_{fu}}{\Gamma \left(1 + \frac{1}{m} \right)} \quad (3b)$$

where σ_{bu} is the tensile strength of fiber bundle, f_L is the volume fraction of longitudinal fiber bundle ($f_L \approx f/2$), σ_{fu} is in situ fiber strength, m is the Weibull modulus of fiber, e is the base of the natural logarithm and Γ is the gamma function.

The predicted values are listed in Table 2 to compare with the measured ones. For the Hi-Nicalon/BN/SiC, the predicted values nearly coincide with the experimental results for all the test temperatures. The consistency indicates that the tensile strength is governed by fiber properties and that the full potential of the fibers is utilized in the composite. This means that the matrix cracking reached a full-saturated state prior to failure, showing a noncatastrophic fracture mode (Figs. 3, 6 and 7) that belongs to a global load sharing (GLS) condition resulting from the lower interface shear stress (Table 3). On the contrary, for the Nicalon/C/SiC, the predicted values are higher than the measured values; in particular, at 1200 K this discrepancy is considerably noticeable. Although the fibrous fracture surfaces are observed [Fig. 7(a) and (b)], there is only a modest amount of fiber pulled-out in the composite, especially at 1200 K where the brittle fracture surface is found. In addition, there are regions in all the bundles in which the fiber-fracture locations are essentially coplanar with another, indicating a strong correlation between breaks. This strong correlation probably results from local strong fiber/matrix bonding. Previous studies revealed that the fiber/matrix debonding in CVI-processed Nicalon/BN/C/SiC is controlled by the thin silica layer resulting from the changes that have occurred near the surface of the metastable Nicalon SiC fiber during processing.^{28,29} Although in the present study the Nicalon/C/SiC was processed by using non-CVI process but PIP process, this thin silica layer is expected to be present at the interface, in particular, for the composite specimens tested above 700 K oxidation of the C-coating promoted formation of silica layer resulting from oxidation of both the matrix and fiber.^{22,23} The interface generated by the silica layer might be the weakest link in the interfacial phase sequence. This silica layer formed during processing or/and oxidation generally is discontinuities and may be regarded as surface flaws which locally weaken the fibers.^{28,29} In the case of the weakest link, fracture of composite is no longer dominated by

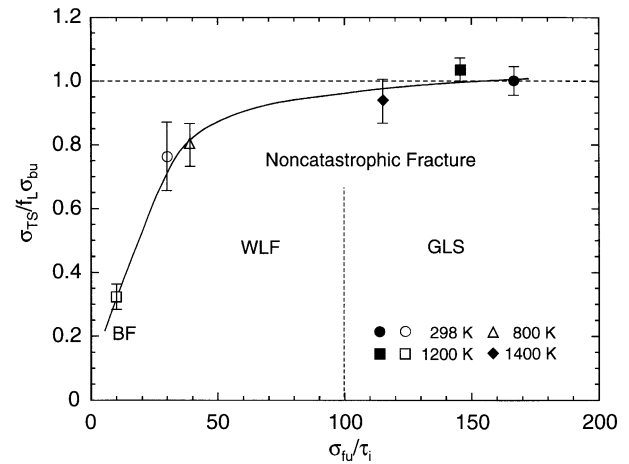


Fig. 8. Correlation of tensile strength of the composites normalized by the predicted values to in situ fiber strength and interface shear stress (BF: brittle fracture, solid symbols: Hi-Nicalon/BN/SiC, dotted symbols: Nicalon/C/SiC).

the fiber bundle strength and ultimate fracture strength is lower than that predicted by fiber bundle model. Therefore, although the Nicalon/C/SiC exhibits a non-linear/noncatastrophic behavior in tension, this composite failed prematurely as compared to the Hi-Nicalon/BN/SiC (Figs. 2 and 3).

Fig. 8 shows correlation of tensile strength and fracture behavior of the both composites to fiber strength and interface shear stress. It is found that the curve could be divided into two characteristic regimes: (i) $\sigma_{fu}/\tau_i \geq 100$, tensile strength of the composite coincides with the values predicted by fiber strength with a noncatastrophic fracture under GLS condition, and (ii) $\sigma_{fu}/\tau_i < 100$, tensile strengths of the composite are lower than the predicted values; typically, as σ_{fu}/τ_i is higher (typical $\sigma_{fu}/\tau_i \geq 30$), the tensile strength of composite is $\sim 80\%$ of predicted value (Table 2) with a weakest link failure (WLF) mode; in particular as σ_{fu}/τ_i is lower (typical $\sigma_{fu}/\tau_i \leq 10$), the tensile strength is only 30% of the predicted value (Table 2) with a brittle fracture fashion. This suggests that the full potential of the fibers is utilized only when the ratio of the interface shear stress to the fiber strength is below a critical value. In the present work, the critical ratio is approximately 1/100.

5. Conclusions

1. For the Nicalon/C/SiC, Young's modulus, tensile strength and strain to failure remained nearly constant up to 800 K and significantly then decreased at 1200 K. A noncatastrophic fracture was observed at and below 800 K, while a brittle fracture fashion similar to monolithic ceramics occurred at 1200 K.

2. For the Hi-Nicalon/BN/SiC, tensile strength and strain to failure increased slightly with increasing test temperature from 298 to 1200 K and then decreased at 1400 K, while Young's modulus decreased with increasing test temperature. A noncatastrophic fracture was observed for all the test temperatures.
3. In situ constituent properties of both composites were determined by tensile stress-strain curves and fracture surface measurements. The constituent properties of Hi-Nicalon/BN/SiC were superior to those of Nicalon/C/SiC, especially at ≥ 1200 K.
4. The tensile strengths of the Hi-Nicalon/BN/SiC were governed by the fibers and could be predicted using fiber bundle model on base of in situ fiber strength. On the contrary, the fracture of the Nicalon/C/SiC was not be dominated by the fiber bundle, with weakest link failure mode.

Acknowledgements

The authors thank Mr. M. Fujikura and Dr. R. Tanaka, Ultra-High Temperature Materials Research Center Co., Ltd., Japan, for their help in the tensile test. The first author (S.Q.G.) would also like to thank the Japan Society for the Promotion of Science for its financial support of his research in Japan.

References

1. Morscher, G. N., Tensile stress rupture of SiC_f/SiC_m minicomposites with carbon and boron nitride interphases at elevated temperatures in air. *J. Am. Ceram. Soc.*, 1997, **80**(8), 2029–2042.
2. Lipetzky, P., Dvorak, G. J. and Stoloff, N. S., Tensile properties of a SiC_f/SiC composite. *Mater. Sci. Eng.*, 1996, **A216**, 11–19.
3. Singh, D., Singh, J. P. and Wheeler, M. J., Mechanical behavior of SiC(f)/SiC composites and correlation to in situ fiber strength at room and elevated temperatures. *J. Am. Ceram. Soc.*, 1996, **79**(3), 591–596.
4. Shin, D. W. and Tanaka, T., Low-temperature processing of ceramic woven fabric/ceramic matrix composites. *J. Am. Ceram. Soc.*, 1994, **77**(1), 97–104.
5. Takeda, M., Kagawa, Y., Mitsuno, S., Imai, Y. and Ichikawa, H., Strength of Hi-NicalonTM/silicon-carbide-matrix composite fabricated by the multiple polymer infiltration-pyrolysis process. *J. Am. Ceram. Soc.*, 1999, **82**(6), 1579–1581.
6. Lissart, N. and Lamon, J., Damage and failure in ceramic matrix minicomposites: experimental study and model. *Acta Mater.*, 1997, **45**(3), 1025–1044.
7. Curtin, W. A., Theory of mechanical properties of ceramic-matrix composites. *J. Am. Ceram. Soc.*, 1991, **74**(11), 2837–2845.
8. Steyer, T. E., Zok, F. W. and Wall, D. P., Stress rupture of an enhanced nicalon/silicon carbide composite at intermediate temperatures. *J. Am. Ceram. Soc.*, 1998, **81**(8), 2140–2146.
9. Xu, H. H. K., Braun, L. M., Ostertag, C. P., Krause, R. F. and Lloyd, I. K., Failure modes of SiC-fiber/Si₃N₄-matrix composites at elevated temperatures. *J. Am. Ceram. Soc.*, 1995, **78**(2), 388–394.
10. Rice, R. W., *Treatise on Materials Science and Technology*, Vol. II, p. 199. Academic Press, New York, 1978.
11. Thouless, M. D. and Evans, A. G., Effects of pullout on the mechanical properties of ceramic matrix composites. *Acta Metall.*, 1988, **36**, 517–522.
12. Heredia, F. E., Spearing, S. M., Evans, A. G., Mosher, P. and Curtin, W. A., Mechanical properties of continuous-fiber-reinforced carbon matrix composites and relationship to constituent properties. *J. Am. Ceram. Soc.*, 1992, **75**(11), 3017–3025.
13. Takeda, M., Sakamoto, J., Saeki, A. and Ichikawa, H., Mechanical and structural analysis of silicon carbide fiber Hi-nicalon type S. *Ceram. Eng. Sci. Proc.*, 1996, **17**(4–5), 35–42.
14. Thouless, M. D., Sbaizero, O., Sigl, L. S. and Evans, A. G., Effect of interface mechanical properties on pullout in a SiC-fiber-reinforced lithium aluminum silicate glass-ceramic. *J. Am. Ceram. Soc.*, 1989, **72**(4), 525–532.
15. Weibull, W., A statistical distribution function of wide applicability. *J. Appl. Mech.*, 1951, **18**, 293–298.
16. Thouless, M. D. and Evans, A. G., Effect of pull-out on the mechanical properties of ceramic matrix composites. *Acta Metall.*, 1988, **36**, 517–522.
17. Beyerle, D. S., Spearing, S. M., Zok, F. W. and Evans, A. G., Damage and failure in unidirectional ceramic-matrix composites. *J. Am. Ceram. Soc.*, 1992, **75**, 2719–2725.
18. Singh, R. N., Influence of interface shear stress on first-matrix cracking stress in ceramic-matrix composites. *J. Am. Ceram. Soc.*, 1990, **73**(10), 2930–2937.
19. Cao, H. C., Bischoff, E., Sbaizero, O., Ruhle, M., Evans, A. G., Marshall, D. B. and Brennan, J. J., Effect of interfaces on the properties of fiber-reinforced ceramics. *J. Am. Ceram. Soc.*, 1990, **73**(6), 1691–1699.
20. Karandikar, P. G. and Chou, T. W., Damage development and moduli reductions in nicalon-CAS composites under static fatigue and cyclic fatigue. *J. Am. Ceram. Soc.*, 1993, **73**, 1720–1728.
21. Kim, R. Y. and Pagano, N. J., Crack initiation in unidirectional brittle-matrix composites. *J. Am. Ceram. Soc.*, 1991, **74**(5), 1082–1090.
22. Llorca, J., Elices, M. and Celemin, J. A., Toughness and microstructural degradation at high temperature in SiC fiber-reinforced ceramics. *Acta Mater.*, 1998, **46**(7), 2441–2453.
23. Ogbuji, L. U. J. T., *A pervasive mode of oxidative degradation in a SiC–SiC composite*, 1998, **81**(11), 2777–2784.
24. Clark, T. J., Arons, R. M. and Stamatoff, J. B., Thermal degradation of nicalon SiC fibers. *Ceram. Eng. Sci. Proc.*, 1985, **6**(7–8), 576–588.
25. Pysher, D. J., Goretta, K. C., Hodder, R. S. and Tressler, R. E., Strengths of ceramic fibers at elevated temperatures. *J. Am. Ceram. Soc.*, 1989, **72**(2), 284–288.
26. Chollon, G., Pailler, R., Naslain, R. and Olry, P., Structure, composition and mechanical behavior at high temperature of the oxygen-free Hi-Nicalon fiber. In *High-Temperature Ceramic-Matrix Composites II*, Vol. 58. ed. A. G. Evans and R. Naslain. Ceram. Trans., The American Ceramic Society, 1995, pp. 299–304.
27. Coleman, B. D., On the strength of classical fibers, fiberbundles. *J. Mech. Phys. Solids*, 1958, **7**, 60–70.
28. Naslain, R., Dugne, O., Guette, A., Sevely, J., Robin-Brosse, C., Rocher, J. P. and Cotteret, J., Boron nitride interphase in ceramic matrix composites. *J. Am. Ceram. Soc.*, 1991, **74**(10), 2482–2488.
29. Prouhet, S., Camus, G., Labrugere, C., Guette, A. and Martin, E., Mechanical characterization of Si-C(O) fiber/SiC (CVI) matrix composites with a BN-interphase. *J. Am. Ceram. Soc.*, 1994, **77**(3), 649–656.